GLOBAL CHANGE BIOLOGY
BIOENERGY

GCB Bioenergy (2017), doi: 10.1111/gcbb.12451

Hemp (*Cannabis sativa* L.) leaf photosynthesis in relation to nitrogen content and temperature: implications for hemp as a bio-economically sustainable crop

KAILEI TANG[1,2], PAUL C. STRUIK[1], STEFANO AMADUCCI[2], TJEERD-JAN STOMPH[1] and XINYOU YIN[1]

[1]*Centre for Crop Systems Analysis, Department of Plant Sciences, Wageningen University & Research, PO Box 430, Wageningen, 6700 AK, The Netherlands,* [2]*Department of Sustainable Crop Production, Università Cattolica del Sacro Cuore, via Emilia Parmense 84, Piacenza, 29122, Italy*

Abstract

Hemp (*Cannabis sativa* L.) may be a suitable crop for the bio-economy as it requires low inputs while producing a high and valuable biomass yield. With the aim of understanding the physiological basis of hemp's high resource-use efficiency and yield potential, photosynthesis was analysed on leaves exposed to a range of nitrogen and temperature levels. Light-saturated net photosynthesis rate (A_{max}) increased with an increase in leaf nitrogen up to 31.2 ± 1.9 μmol m^{-2} s^{-1} at 25 °C. The A_{max} initially increased with an increase in leaf temperature (T_L), levelled off at 25–35 °C and decreased when T_L became higher than 35 °C. Based on a C_3 leaf photosynthesis model, we estimated mesophyll conductance (g_m), efficiency of converting incident irradiance into linear electron transport under limiting light (κ_{2LL}), linear electron transport capacity (J_{max}), Rubisco carboxylation capacity (V_{cmax}), triose phosphate utilization capacity (T_p) and day respiration (R_d), using data obtained from gas exchange and chlorophyll fluorescence measurements at different leaf positions and various levels of incident irradiance, CO_2 and O_2. The effects of leaf nitrogen and temperature on photosynthesis parameters were consistent at different leaf positions and among different growth environments except for κ_{2LL}, which was higher for plants grown in the glasshouse than for those grown outdoors. Model analysis showed that compared with cotton and kenaf, hemp has higher photosynthetic capacity when leaf nitrogen is <2.0 g N m^{-2}. The high photosynthetic capacity measured in this study, especially at low nitrogen level, provides additional evidence that hemp can be grown as a sustainable bioenergy crop over a wide range of climatic and agronomic conditions.

Keywords: Hemp (*Cannabis sativa* L.), model, nitrogen, photosynthesis, sustainable crop, temperature

Received 27 January 2017; revised version received 4 April 2017 and accepted 12 April 2017

Introduction

The multiple societal challenges such as climate change, natural resource scarcity and environmental pollution have fuelled interest in bio-economy (Jordan *et al.*, 2007). Previous comprehensive research programmes indicated that hemp (*Cannabis sativa* L.) fits well in the concept of bio-economy (Mccormick & Kautto, 2013; Amaducci *et al.*, 2015). Hemp has the potential to produce up to 27 Mg ha^{-1} biomass yield (Tang *et al.*, 2016) at relatively low inputs (Struik *et al.*, 2000; Amaducci *et al.*, 2002) and has a positive impact on the environment (Bouloc & Van der Werf, 2013; Barth & Carus, 2015). Its stem contains high-quality cellulose (De Meijer & Van der Werf, 1994), the seeds contain high-quality oil (Oomah *et al.*, 2002), and the inflorescence contains valuable resins (Bertoli *et al.*, 2010). From speciality pulp and paper to nutritional food, medicine and cosmetics, there are as many as 50 000 uses claimed for hemp products derived from its stem, seed and inflorescence (Carus *et al.*, 2013; Carus & Sarmento, 2016). Recent research demonstrated that hemp is also a suitable feedstock for bioenergy production (Rice, 2008; Kreuger *et al.*, 2011; Prade *et al.*, 2011).

Although once an important crop for the production of textiles and ropes, hemp has not been subjected to the intensive research that has driven great improvements in major crops in the last 50 years (Amaducci *et al.*, 2015; Salentijn *et al.*, 2015) due to the continuous decrease in hemp acreage after the Second World War and its slow revival in the last couple of decades

Correspondence: Xinyou Yin, tel. +31 317482348, fax +31 317485572, e-mail: xinyou.yin@wur.nl

(Wirtshafter, 2004; Allegret, 2013). To advance research needed to consolidate and expand the market of hemp renewable materials, within the frame of the EU funded project Multihemp (www.multihemp.eu), it was proposed to develop a process-based hemp growth model similar to the successful models for major staple crops (Bouman *et al.*, 2007). With the aim of understanding the physiological basis of hemp's high resource-use efficiency and yield potential using a modelling approach, this study focuses on analysing leaf photosynthesis of hemp as a primary source of biomass production.

Very few studies report on leaf photosynthesis of hemp. De Meijer *et al.* (1995) reported a light-saturated rate of leaf photosynthesis for hemp of 30 kg CO_2 ha^{-1} h^{-1} (equivalent to 19 μmol m^{-2} s^{-1}) under field conditions. Chandra *et al.* (2008, 2011a,b, 2015) showed the response of leaf photosynthesis of hemp to irradiance intensity, CO_2 concentration and temperature by measuring gas exchange of leaves from glasshouse-grown plants. Marija *et al.* (2011) found that nitrogen fertilization significantly affected different aspects of photosynthetic photochemistry, as shown by chlorophyll *a* fluorescence analysis. To the best of our knowledge, a comprehensive analysis of the relation between leaf nitrogen status and photosynthesis rate is not yet available for hemp.

Leaf photosynthesis rate depends on both nitrogen nutrition status and environmental conditions (Sinclair & Horie, 1989). Thanks to a thorough understanding of the biochemical mechanisms of leaf photosynthesis, the response of leaf photosynthesis to irradiance intensity and CO_2 concentration can be modelled (Farquhar *et al.*, 1980; Yin *et al.*, 2006; Von Caemmerer *et al.*, 2009). Such a model dissects net leaf photosynthesis into mesophyll conductance (g_m), linear electron transport capacity (J_{max}), Rubisco carboxylation capacity (V_{cmax}), triose phosphate utilization capacity (T_p) and day respiration (R_d). The effects of leaf nitrogen status and temperature on leaf photosynthesis are considered through their effects on these photosynthetic parameters (Hikosaka *et al.*, 2016). Experimental protocols for parameterizing the biochemical photosynthesis model have been well documented (Sharkey *et al.*, 2007; Yin *et al.*, 2009; Bellasio *et al.*, 2015), and the model has been successfully embedded as a submodel in process-based crop growth models for upscaling to canopy photosynthesis and crop production (Yin & Struik, 2009), such as the GECROS crop model (Yin & Van Laar, 2005). Therefore, parameterizing the photosynthesis model for hemp is an excellent opportunity to understand its photosynthetic resource-use efficiency, as well as to provide essential information for modelling hemp growth.

The first objective of this study was to analyse leaf photosynthesis of hemp as affected by irradiance intensity, CO_2 concentration, temperature and nitrogen status. Secondly, this study aimed to parameterize a widely used C_3 leaf photosynthesis model (Farquhar *et al.*, 1980; Yin *et al.*, 2006) for hemp. In the final section, the photosynthetic capacity of hemp is compared with that of two other bio-economic crops, cotton (*Gossypium hirsutum* L.) and kenaf (*Hibiscus cannabinus* L.), using a modelling method. Cotton and kenaf were chosen because they are bio-economically important crops and, in particular, kenaf is considered as an alternative for hemp in tropical and subtropical climates (Lips & van Dam, 2013; Patanè & Cosentino, 2013; Alexopoulou *et al.*, 2015).

Materials and methods

Plant growth and data collection

Three independent experiments were carried out at the research facilities of the Università Cattolica del Sacro Cuore (45.0°N, 9.8°E, 60 m asl; Piacenza, Italy). Seeds of hemp (*cv.* Futura 75) were received from the Fédération National des Producteurs de Chanvre, Le Mans, France. The plants were grown outdoors in 2013 and 2014 and in a glasshouse in 2015.

An experiment on the effect of nitrogen on leaf photosynthetic capacity (N-trial)

Seeds were sown in 18 containers (40 × 40 × 30 cm^3) placed outdoors on 9 May 2014. Each container was filled with 23 kg of soil (dry weight) that contained 0.22% total nitrogen and had a clay–silt–sand ratio of 30:43:27. After seedling emergence, the plants were hand-thinned to 18 plants per container and three levels of urea fertilization were applied (0, 1.0 and 2.0 g N per container, respectively). There were six containers for each fertilization level. Other nutrients (e.g. phosphate and potassium) were assumed not limiting factors according to historic experience in the field from which the soil was collected. The same applies to the other two trials. During plant growth, all containers were positioned randomly and tightly in one block surrounded by a green shading net (transmitting 3% of the light). The net height was adjusted daily according to the increment of plant height. The plants were well watered during the entire experiment. The daily temperature and global radiation during the growth period are presented in Fig. S1.

Photosynthetic measurements were started on 46 days after sowing (the 6th–8th pair of leaves had appeared) in a growth chamber with the temperature set at 25 °C. The container was moved into the growth chamber 2 hrs before measurements. On one representative plant in each container, the middle leaflets of the youngest, fully expanded top leaf and of the middle leaf (i.e. two nodes below the top leaf) were measured. Simultaneous gas exchange (GE) and chlorophyll fluorescence (CF) measurements were implemented *in situ* using a portable open gas exchange system with a 1.7-cm^2 clamp-on leaf chamber (CIRAS-2, PP Systems international, Inc., Amesbury, MA, USA)

 doi: 10.1111/gcbb.12451

combining with FMS2 (Hansatech Instruments Ltd, King's Lynn, Norfolk, UK). The system set-up of the combined CIRAS-2 and FMS2 for performing simultaneous GE and CF measurements was implemented according to the instructions provided by PP Systems International, Inc., USA. Light response curve of net photosynthesis rate (A) (A-I_{inc}) and its CO_2 response curve (A-C_a) were assessed for each leaf under ambient O_2 (i.e. 21%) conditions. The A-I_{inc} curves were assessed by decreasing incident light intensity (I_{inc}) as 2000, 1500, 1000, 500, 300, 200, 150, 100, 60 and 30 μmol m^{-2} s^{-1}, while keeping leaf chamber CO_2 concentration (C_a) at 400 μmol mol^{-1}. At the end of assessing the A-I_{inc} curve, the light source was turned off for 15 min to measure leaf respiration in darkness (R_{dk}). The A-C_a curves were assessed by changing C_a as 400, 250, 150, 80, 70, 60, 50, 400, 400, 600, 800, 1000 and 1500 μmol mol^{-1}, while keeping I_{inc} at 1000 μmol m^{-2} s^{-1}. Leaf temperature (T_L) and vapour pressure of supplying air during measurements were set constant at 25 °C and 2 kPa, respectively. The response curves were started when the leaf had adapted to the condition at the first I_{inc} or C_a level for 30 min. Data were recorded programmatically with 2-min interval for A-I_{inc} curves and 3-min interval for A-C_a curves. Premeasurements indicated these time intervals were sufficiently long for A to reach a steady state. Three plants were measured for each fertilization level.

To obtain a calibration factor that can properly convert fluorescence-based PSII efficiency into linear electron transport rate, parts of A-I_{inc} and A-C_a curves were also assessed under 2% O_2. This condition was realized by supplying the CIRAS-2 with a humidified mixture of 2% O_2 and 98% N_2. To avoid O_2 leakage, the air-in pump in the CIRAS-2 was replaced by a sealed one according to the manufacturer's instruction. The curves for 2% O_2 were assessed in accordance with the ones for ambient O_2, but the A-I_{inc} curves were only assessed at I_{inc} ≤150 μmol m^{-2} s^{-1} and the A-C_a curves were only assessed at C_a ≥600 μmol mol^{-1}. These particular I_{inc} and C_a conditions are required for obtaining the calibration factor (Yin *et al*., 2009), that is to ensure that A is limited by electron transport.

When the photosynthetic measurements were completed, *SPAD*, a proxy for chlorophyll concentration, was measured using a SPAD-502 (Minolta, Japan). Leaf area was determined from scans using IMAGEJ (version 1.49; https://imagej.nih.gov/). Dry weight was measured after drying at 75 °C until constant weight. Total leaf nitrogen concentration was analysed using a *CN* analyser (Vario Max CN Analyzer; Elementar Americas, Inc., Hanau, Germany). Specific leaf nitrogen (*SLN*; g N m^{-2}) was calculated for each measured leaf using the leaf dry weight, leaf area and nitrogen concentration. CO_2 leakage of the CIRAS-2 leaf chamber was assessed by performing A-C_a curves on three heat-killed leaves. Based on these measurements, values of A and the intercellular CO_2 concentration (C_i) of A-C_a curves were recalculated using the CIRAS-2 built-in formulae.

An experiment on the effect of temperature on leaf photosynthetic capacity (T-trial)

Seeds were sown in six pots (10 × 10 × 15 cm^3) placed in a glasshouse on 12 February 2015. Each pot contained 1 kg of soil that had identical properties with the ones in the N-trial. The temperature in the glasshouse was maintained at approximately 25 °C. A LED lamp (270 Watt, Shenzhen GTL Lighting Co., Ltd, China) mounted 50 cm above the canopy for 16 hrs each day gave the light level in glasshouse of approximately 600 μmol m^{-2} s^{-1}. After emergence, the plants were hand-thinned to two plants per pot, and urea fertilization was applied (0.3 g N per pot). The plants were well watered during growth.

Starting on 46 days after sowing, GE measurements were conducted in a temperature-controllable chamber. On one plant in each pot, the middle leaflet of the youngest, fully expanded top leaf was measured. The A-I_{inc} and A-C_a curves were assessed subsequently at T_L 15, 20, 25, 30, 35 and 40 °C. The levels of I_{inc} and C_a were set in accordance with the N-trial under ambient O_2. During the measurements, the temperature in the growth chamber was controlled close to the targeting T_L and the vapour pressure of supplying air was set at 1.5 kPa for all temperature levels except for 15 °C, when it was set at 1.0 kPa to avoid water condensation. Three plants were measured. *SPAD*, *SLN* and gas leakage were analysed using the procedures described for the N-trial.

An experiment on leaf photosynthesis in response to fluctuating temperature under different leaf nitrogen levels (TN-trial)

Seeds were sown in 18 containers (60 × 20 × 18 cm^3) placed outdoor on 5 August 2013. Each container was filled with 10 kg of soil that contained 0.11% of total nitrogen and had a clay–silt–sand ratio of 15:22:63. After seedling emergence, the plants were hand-thinned to 10 plants per container and three levels of urea fertilization were applied (0, 0.78 and 1.95 g N per container, respectively). Each fertilization level had six containers. The plants were well watered during growth. Because of very late sowing, a halogen lamp (54 Watt) that was mounted at 50 cm from the top of canopy was turned on for 16 hrs per day to prevent plants from flowering. The daily temperature and radiation during the growth period are presented in Fig. S1.

Starting on 50 days after sowing (the 8th – 10th pair of leaves had appeared), GE measurements were conducted outdoors on three representative plants for each nitrogen level. A-I_{inc} and A-C_a curves were assessed on the middle leaflet of the youngest, fully expanded leaf. The levels of light for the A-I_{inc} curves were identical to those in the N-trial under ambient O_2, while the A-C_a curves were assessed by increasing C_a as: 50, 60, 70, 80, 150, 250, 400, 650, 1000 and 1500 μmol mol^{-1} while keeping I_{inc} at 1000 μmol m^{-2} s^{-1}. During measurement, T_L and vapour pressure were not controlled and, therefore, varied depending on ambient conditions. A response curve was started when the leaf had adapted to the leaf chamber for 15 min at the first I_{inc}/C_a level. Data were recorded manually when the real-time net photosynthesis (A) had apparently reached steady state (~ 3 min for A-I_{inc} and ~ 5 min for A-C_a). *SPAD*, *SLN* and gas leakage were analysed using the procedures described for the N-trial.

 doi: 10.1111/gcbb.12451

Model analysis

The photosynthesis model of Farquhar *et al.* (1980) coupled with CO_2 diffusion model, as described in Yin & Struik (2009), was used in this study.

Modelling net leaf photosynthesis rate at the carboxylation sites of Rubisco

The net leaf photosynthesis rate (A, μmol m^{-2} s^{-1}) was modelled as the minimum of the Rubisco-limited rate (A_c), the electron transport-limited rate (A_j) and the triose phosphate utilization-limited rate (A_p):

$$A = \min(A_c, A_j, A_p) \quad (1)$$

A_c is described, following the Michaelis–Menten kinetics, as:

$$A_c = \frac{(C_c - \Gamma^*)V_{cmax}}{C_c + K_{mc}(1 + O/K_{mo})} - R_d \quad (2)$$

where C_c (μmol mol^{-1}) and O (mmol mol^{-1}) are the CO_2 and O_2 levels at the carboxylation sites of Rubisco; V_{cmax} (μmol m^{-2} s^{-1}) is the maximum rate of carboxylation; K_{mc} (μmol mol^{-1}) and K_{mo} (mmol mol^{-1}) are Michaelis–Menten constants of Rubisco for CO_2 and O_2, respectively; R_d (μmol m^{-2} s^{-1}) is the day respiration (respiratory CO_2 release other than by photorespiration); and Γ^*(μmol mol^{-1}) is the CO_2 compensation point in the absence of R_d.

A_j is described as:

$$A_j = \frac{(C_c - \Gamma^*)J}{4C_c + 8\Gamma^*} - R_d \quad (3)$$

where J (μmol m^{-2} s^{-1}) is the potential linear e^- transport rate that is used for CO_2 fixation and photorespiration, and it is described as:

$$J = \frac{\kappa_{2LL}I_{inc} + J_{max} - \sqrt{(\kappa_{2LL}I_{inc} + J_{max})^2 - 4\theta J_{max}\kappa_{2LL}I_{inc}}}{2\theta} \quad (4)$$

where J_{max} (μmol m^{-2} s^{-1}) is the maximum value of J under saturated light; I_{inc} is the incident light (μmol m^{-2} s^{-1}); κ_{2LL} (mol mol^{-1}) is the conversion efficiency of incident light into J at strictly limiting light; and θ (dimensionless) is convexity factor for the response of J to I_{inc}.

A_p is described as:

$$A_p = 3T_p - R_d \quad (5)$$

where T_p (μmol m^{-2} s^{-1}) is the rate of triose phosphate export from the chloroplast.

The T_L response of R_d, T_p and kinetic properties of Rubisco (involving V_{cmax}, K_{mc}, K_{mo} and Γ^*) are described using an Arrhenius function normalized with respect to their values at 25 °C (Eqn 6) while the response of J_{max} is described using a peaked Arrhenius function (Eqn 7):

$$X = X_{25}\exp\left[\frac{E_x(T_L - 25)}{298R(T_L + 273)}\right] \quad (6)$$

$$X = X_{25}\exp\left[\frac{E_x(T_L - 25)}{298R(T_L + 273)}\right]\left[\frac{1 + \exp\left(\frac{298S_x - D_x}{298R}\right)}{1 + \exp\left(\frac{(T_L+273)S_x - D_x}{R(T_L+273)}\right)}\right] \quad (7)$$

where X_{25} is the value of each parameter at 25 °C (i.e. R_d, V_{cmax}, K_{mc}, K_{mo}, Γ^* and J_{max}). E_x and D_x are the energies of activation and deactivation (i.e. E_{Rd}, E_{Vcmax}, E_{Kmc}, E_{Kmo}, E_{Tp}, E_{Γ^*}, E_{Jmax} and D_{Jmax}, all in J mol^{-1}); S_x is the entropy term (S_{Jmax} in J K^{-1} mol^{-1}); and R is the universal gas constant (=8.314 J K^{-1} mol^{-1}).

Modelling mesophyll conductance for CO_2

The CO_2 concentration at intercellular space (C_i) was taken from gas exchange measurement whereas the estimation of C_c relies on proper estimation of mesophyll conductance (g_m). g_m, calculated by the variable J method (Harley *et al.*, 1992a), appeared to vary with CO_2 and irradiance levels (see section Result). Whether or not g_m varies with CO_2 and irradiance levels is debatable (Flexas *et al.*, 2007, 2012). We used the model of Yin *et al.* (2009) that is able to deal with both constant and variable g_m models, and have a similar form as Eqn (8):

$$g_m = g_{m0} + \frac{\delta(A + R_d)}{C_c - \Gamma^*} \quad (8)$$

where g_{m0} (mol m^{-2} s^{-1}) is the minimum g_m if irradiance approaches zero; parameter δ (dimensionless) in this model defines the $C_c : C_i$ ratio at saturating light as $(C_c - \Gamma^*)/(C_i - \Gamma^*) = 1/(1 + 1/\delta)$. Any positive value of δ predicts a variable g_m pattern in response to C_i and I_{inc}, and a higher δ implies higher g_m and therefore a higher $C_c : C_i$ ratio. If $\delta = 0$, Eqn (8) predicts an independence of g_m on C_i and I_{inc} (i.e. $g_m = g_{m0}$), equivalent to the constant-g_m model.

Model parameterization and validation

The data collected in the N-trial was used to assess the effect of leaf nitrogen on the values of model parameters at 25 °C. The data collected in the T-trial were used to assess the effect of leaf temperature on the values of (peaked) Arrhenius model parameters. The parameterized model was validated against the data collected in the TN-trial. In the model, Rubisco kinetic property-related parameters (i.e. K_{mc}, K_{mo} and Γ^*) and θ, convexity factor for the response of J to I_{inc}, are conserved among C_3 species (Von Caemmerer *et al.*, 2009). Thus, the value of θ was set to 0.7 (Ögren & Evans, 1993); the values of K_{mc}, K_{mo} and Γ^* at 25 °C were set to 272 μmol mol^{-1}, 165 mmol mol^{-1} and 37.5 μmol mol^{-1} (at 21% O_2), respectively (Bernacchi *et al.*, 2002). The energies of activation E_{Kmc}, E_{Kmo} and E_{Γ^*} were adapted from the values of Bernacchi *et al.* (2002) as E_{Kmc} = 80990 J mol^{-1}, E_{Kmo} = 23720 J mol^{-1} and E_{Γ^*} = 24460 J mol^{-1}.

Model parameterization with data collected in the N-trial: nitrogen effect

The stepwise parameterizing procedures described by Yin *et al.* (2009) were adapted in this study. Specifically:

Step 1: Estimating electron transport parameters (J_{max} and κ_{2LL}) and R_d

According to Yin *et al.* (2009), the observed A_j under non-photorespiratory conditions can be expressed using Eqn (9):

$$A_j = \frac{sI_{inc}\Phi_2}{4} - R_d \tag{9}$$

$$s = \beta\rho_2\left(1 - \frac{f_{pseudo(b)}}{1 - f_{cyc}}\right) \tag{9a}$$

where s is a lumped parameter; Φ_2 is PSII operating efficiency, usually assessed from the chlorophyll fluorescence measurements, indicating quantum efficiency of PSII e^- flow on PSII-absorbed light basis; β is leaf absorptance; ρ_2 is proportion of absorbed I_{inc} partitioned to PSII; and f_{cyc} and $f_{pseudo(b)}$ are the fraction of cyclic and basal pseudocyclic electron transport, respectively. Thus, a simple linear regression can be performed for the observed A against $(I_{inc}\Phi_2/4)$ using data of the e^- transport-limited range under nonphotorespiratory conditions (measurements conducted at 2% O_2). The slope of the regression yields an estimate of the calibration factor s, and the intercept gives an estimate of R_d under 2% O_2 condition. The estimated s allowed the conversion of CF-based PSII operating efficiency into the actual rate of linear electron transport as:

$$J = sI_{inc}\Phi_2 \tag{10}$$

Thus, J_{max} and κ_{2LL} can be estimated from fitting Eqn (4) to the values of J.

The same linear regression for the observed A against $(I_{inc}\Phi_2/4)$ using data of the e^- transport-limited range may be applied as well to photorespiratory conditions (i.e. ambient O_2) for estimating R_d although the slight variation in C_i with I_{inc} can have bearing under these conditions (Yin *et al.*, 2009, 2011).

Step 2: Parameterization of the g_m model and V_{cmax} and T_p

Combining Eqn (8) with Eqn (2) and Eqn (3), and replacing C_c with $(C_i - A/g_m)$ yields (Yin *et al.*, 2009):

$$A_c \text{ or } A_j = \frac{-b - \sqrt{b^2 - 4ac}}{2a} \tag{11}$$

where

$$a = x_2 + \Gamma^* + \delta(C_i + x_2)$$

$$b = -\Big\{(x_2 + \Gamma^*)\,(x_1 - R_d) + (C_i + x_2)[g_{m0}(x_2 + \Gamma^*) + \delta(x_1 - R_d)] + \delta[x_1(C_i - \Gamma^*) - R_d(C_i + x_2)]\Big\}$$

$$c = \big[g_{m0}(x_2 + \Gamma^*) + \delta(x_1 - R_d)\big][x_1(C_i - \Gamma^*) - R_d(C_i + x_2)]$$

$$\text{with } x_1 = \begin{cases} V_{cmax} & \text{for} A_c \\ \frac{J}{4} & \text{for} A_j \end{cases}$$

$$\text{and } x_2 = \begin{cases} K_{mc}\left(1 + \frac{O}{K_{mo}}\right) & \text{for} A_c \\ 2\Gamma^* & \text{for } A_j \end{cases}$$

Thus, V_{cmax}, T_p and δ (or g_{m0}) can be estimated simultaneously by fitting Eqn (1), Eqn (4), Eqn (5) and Eqn (11) to A-I_{inc} and A-C_i using pre-estimated J_{max}, κ_{2LL} and R_d as input.

As it is uncertain if g_m varies with CO_2 and irradiance levels, g_m was first assessed according to the variable J method (Harley *et al.*, 1992a):

$$g_m = \frac{A}{C_i - \frac{\Gamma^*[J + 8(A + R_d)]}{J - 4(A + R_d)}} \tag{12}$$

where A and C_i were taken from gas exchange measurements and J was calculated by Eqn (10). If g_m does vary in response to changing C_i and I_{inc}, we could fit only δ by fixing g_{m0} to 0 (Yin *et al.*, 2009). In such a case, g_m can be calculated as:

$$g_m = \frac{A + \delta(A + R_d)}{C_i - \Gamma^*}. \tag{13}$$

Model parameterization with data collected in the T-trial: temperature effect

By assuming the value of δ is independent of leaf temperature, the values of J_{max}, κ_{2LL}, V_{cmax} and T_p at each leaf temperature were solved from Eqn (1), Eqn (4), Eqn (5) and Eqn (11) by simultaneously fitting A-I_{inc} and A-C_i curves. Subsequently, the parameter values at different T_L were fitted to either Eqn (6) for estimating E_{Rd}, E_{Vcmax}, E_{Tp}, or Eqn (7) for estimating E_{Jmax}, D_{Jmax} and S_{Jmax}.

Model validation

The parameterized model was validated against the data obtained in the TN-trial. The model parameters R_d, J_{max}, V_{cmax} and T_p at 25 °C were derived from their linear relationships with *SLN* (see section Result), and the effect of T_L on the values of these parameters was quantified through Eqn (6) or Eqn (7) with the estimated E_{Rd}, E_{Vcmax}, E_{Tp}, E_{Jmax}, D_{Jmax} and S_{Jmax}.

Comparison of hemp leaf photosynthetic competence with that of cotton and kenaf

To illustrate the leaf photosynthetic competence of hemp in comparison with cotton and kenaf, A-C_i, A-I_{inc}, A-T_L and *A-SLN* curves were constructed for hemp using the validated model while those of cotton and kenaf were constructed using the FvCB models and corresponding parameters reported in Harley *et al.* (1992b) for cotton (*cv.* Coker 315) and in Archontoulis *et al.* (2011) for kenaf (*cv.* Everglades 41).

Statistics

Simple linear regression was performed using Microsoft Excel. Nonlinear fitting was carried out using the GAUSS method in PROC NLIN of SAS (SAS Institute Inc., Cary, NC, USA). If parameters were proven independent from leaf nitrogen or temperature, the dummy variables method was used to estimate one common value (Yin *et al.*, 2009). The goodness of fit was assessed by calculating the coefficient of determination (r^2) and the relative root mean square (*rRMSE*). The effect of leaf position on parameter values was tested by performing ANOVA test considering leaf nitrogen as covariance.

 doi: 10.1111/gcbb.12451

Results

Results of the N-trial: nitrogen-dependent photosynthetic capacity

Measurements to assess the effect of leaf nitrogen on leaf photosynthetic capacity of hemp (N-trial) were conducted on leaves having an average *SLN* of 0.87 g N m^{-2}, 1.25 g N m^{-2} and 1.75 g N m^{-2} at the top of the canopy, or 0.65 g N m^{-2}, 0.78 g N m^{-2} and 1.22 g N m^{-2} at the middle of the canopy, for the three N treatments, respectively. Examples of A-I_{inc} and A-C_i curves at different *SLN* levels are shown in Fig. 1. The R_{dk} (μmol m^{-2} s^{-1}; leaf respiration in the dark) and light-saturated net photosynthesis rate (A_{max}; measured at 2000 μmol m^{-2} s^{-1}) increased linearly with increasing *SLN*, and these linear relationships did not differ between the top and middle leaves (Fig. 2).

Using the data of electron transport-limited range under nonphotorespiratory conditions (i.e. at 2% O_2, C_a ≥600 μmol mol^{-1} in the A-C_a curve and I_{inc} ≤150 μmol m^{-2} s^{-1} in the A-I_{inc} curve), parameter s was estimated as the slope of a linear regression of A against ($I_{inc}\Phi_2$/4). The value of s was independent of *SLN* and canopy position ($P > 0.05$; see Fig. S2a). Thus, a common s (0.33 ± 0.01) was estimated from pooled data. κ_{2LL} and J_{max} were estimated from fitting Eqn (4) to the data on calculated J from Eqn (10). A preliminary estimation indicated that κ_{2LL} was unlikely to change with *SLN* and canopy position ($P > 0.01$; Fig. S2b). Thus, a common κ_{2LL} (0.21 ± 0.004 mol mol^{-1}) was estimated together with J_{max} using the dummy variable method. The J_{max} ranged from 116.1 μmol m^{-2} s^{-1} to 316.4 μmol m^{-2} s^{-1} and increased linearly with an increase in *SLN* at the rate of 132.9 μmol s^{-1} (g N)$^{-1}$ (Fig. 3a). The relationship between J_{max} and *SLN* was independent of canopy position ($P > 0.05$).

The estimated R_d values at 21% O_2 were roughly in line with the ones at 2% O_2 (see Fig. S3). Although the latter were on average 25% lower, a test of covariance indicated that R_d did not differ significantly between the different O_2 levels ($P = 0.17$). At 21% O_2, R_d ranged from 0.29 μmol m^{-2} s^{-1} to 1.61 μmol m^{-2} s^{-1}, increasing linearly with *SLN* at a rate of 0.85 μmol s^{-1} (g N)$^{-1}$ (Fig. 3b). The R_d-*SLN* relationship did not differ much between the middle and top leaves ($P > 0.05$).

The g_m calculated using the variable J method, Eqn (12), indicated that it varied with changing I_{inc} and C_i (Fig. 4a, b). A preliminary analysis indicated that the value of g_{m0} in Eqn (8) was close to zero. By fixing g_{m0} to zero, a common value of δ (2.12 ± 0.09) was estimated together with V_{cmax} and T_p using the dummy variable method. With the estimated δ, Eqn (13) estimates that g_m changes with I_{inc} and C_i in a similar trend as observed for the g_m calculated using Eqn (12); the latter, however, was 38% lower (Fig. 4a, b), probably as a result that the variable J method assumes the limitation on photosynthesis by electron transport over the full range of A-I_{inc} and A-C_i curves (Yin *et al.*, 2009). The estimated g_m with Eqn (13) increases with an increase in *SLN* (Fig. 4c). The estimated V_{cmax} ranged from 53.7 μmol m^{-2} s^{-1} to 163.2 μmol m^{-2} s^{-1} and increased linearly with an increase in *SLN* at the rate of 76.2 μmol s^{-1} (g N)$^{-1}$ (Fig. 3c). The estimated T_p ranged from 6.9 μmol m^{-2} s^{-1} to 11.5 μmol m^{-2} s^{-1} and increased linearly with an increase in *SLN* at the rate of 4.2 μmol s^{-1} (g N)$^{-1}$ (Fig. 3d). The effects of *SLN* on V_{cmax} and T_p were independent of leaf position ($P > 0.05$). With the estimated R_d, κ_{2LL}, J_{max}, δ, V_{cmax} and T_p, the r^2 and *rRMSE* of the model description of the measured A in the N-trial were 0.99 and 18.5%, respectively.

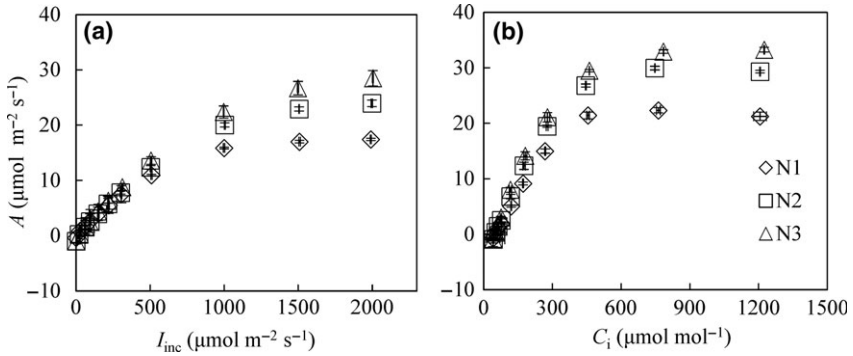

Fig. 1 The net leaf photosynthesis (A) in response to incident irradiance (I_{inc}; Panel a) and intercellular CO_2 concentration (C_i; Panel b) under different leaf nitrogen levels. Data presented were measured at 21% O_2 on the top leaves in the N-trial. N1, N2 and N3 correspond to nitrogen treatments, resulting in average specific leaf nitrogen values of 0.87 g N m^{-2}, 1.25 g N m^{-2} and 1.75 g N m^{-2}, respectively. The bars indicate standard errors of the mean ($n = 3$).

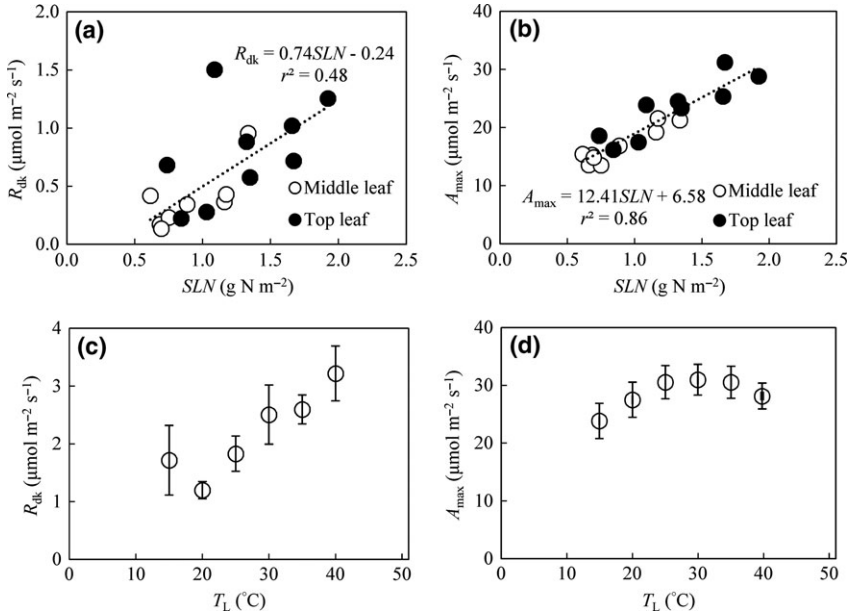

Fig. 2 The response of leaf respiration in dark (R_{dk}, panels a and c) and maximum light-saturated net photosynthesis rate (A_{max}; panels b and d) to specific leaf nitrogen (*SLN*; panels a and b) and leaf temperature (T_L; panels c and d). R_{dk} was measured after adapting leaves in dark for 15 min after measuring the A - I_{inc} curve. A_{max} was measured at 2000 μmol m^{-2} s^{-1} for incident light intensity and 400 μmol mol^{-1} for ambient CO_2 concentration. The data presented in Panel a and Panel b were obtained in the N-trial while those in Panel c and Panel d were obtained in the T-trial. The bars in panels c and d indicate standard errors of the mean (n = 3).

Results of T-trial: temperature-dependent photosynthetic capacity

The R_{dk} increased continuously from 0.9 μmol m^{-2} s^{-1} to 4.1 μmol m^{-2} s^{-1} at increasing T_L from 15 to 40 °C while the A_{max} initially increased with increasing T_L, levelled off at 25–35 °C and decreased when T_L became higher than 35 °C (Fig. 2c, d).

The estimated R_d increased continuously with an increase in T_L, ranging from 0.3 μmol m^{-2} s^{-1} until 3.2 μmol m^{-2} s^{-1} (Fig. 5a). The κ_{2LL}, J_{max}, V_{cmax} and T_p were estimated simultaneously by assuming δ = 2.12 (estimated in N-trial) at each T_L. With the constant δ, the model predicted that g_m changed with an increase in T_L following a similar trend as A_{max} (cf. Figs 2d and 4d). A preliminary analysis indicated that κ_{2LL} was conserved at different levels of T_L (P > 0.05; see Fig. S2c) but significantly higher than the value estimated in the N-trial (i.e. κ_{2LL} = 0.21 ± 0.004 mol mol^{-1}). Thus, a common κ_{2LL} (0.37 ± 0.01 mol mol^{-1}) was estimated together with J_{max}, V_{cmax} and T_p using the dummy variable method. The J_{max}, V_{cmax} and T_p at 25 °C were comparable with those derived from the N-trial (Fig. 3). The value of T_p increased consistently with an increase in T_L from 15 to 30 °C (Fig. 5d). When T_L was higher than 30 °C, the curve fitting failed to assess T_p properly because the triose phosphate utilization is not limited at such high temperatures (Sage & Kubien, 2007; Busch & Sage, 2016). Therefore, T_p limitation was excluded to estimate J_{max} and V_{cmax} at 35 and 40 °C. The V_{cmax} increased continuously at increasing T_L from 15 to 40 °C while the value of J_{max} peaked at 30–35 °C (Fig. 5b, c).

By fitting the R_d-T_L, V_{cmax}-T_L and T_p-T_L to Eqn (6), the activation energies E_{Rd}, E_{Vcmax} and E_{Tp} were estimated at 21634.8 ± 4085.5 J mol^{-1}, 63042.7 ± 1562.2 J mol^{-1} and 34417.8 ± 5297.7 J mol^{-1}, respectively. By fitting J_{max}-T_L to Eqn (7), the values of E_{Jmax}, D_{Jmax} and S_{Jmax} were estimated at 67292.1 ± 35985.5 J mol^{-1}, 114701.0 ± 28709.6 J mol^{-1} and 375.6 ± 82.3 J K^{-1} mol^{-1}, respectively. With the estimated parameters, the model described well the response of A to changing I_{inc} and C_i at different T_L (r^2 = 0.94 and $rRMSE$ = 24.1%).

Model validation

The measurements in the TN-trial were conducted on leaves with *SLN* ranging from 0.63 g N m^{-2} to 1.44 g N m^{-2}. During the measurement, the T_L ranged from 21 to 33 °C, and *VPD* ranged from 0.61 kPa to 2.61 kPa.

The parameterized model was validated against the data obtained in the TN-trial. The measured A was overestimated with either the κ_{2LL} derived in the N-trial

 doi: 10.1111/gcbb.12451

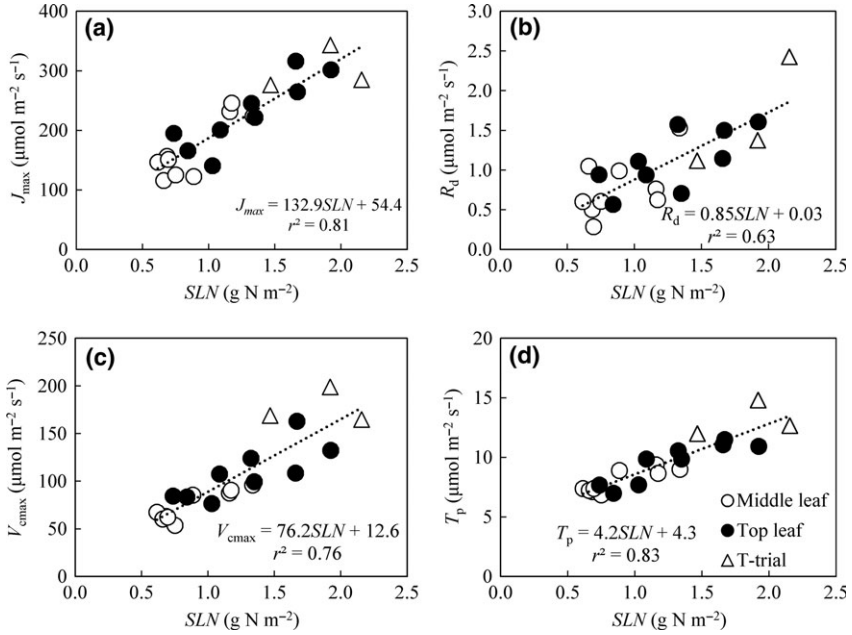

Fig. 3 Dependence of maximum potential linear e$^-$ transport rate (J_{max}; Panel a), day respiration (R_d; Panel b), maximum rate of carboxylation (V_{cmax}; Panel c) and the rate of triose phosphate export from the chloroplast (T_p: Panel d) on specific leaf nitrogen (*SLN*). Values indicated as circles (○ and ● denote leaves at the middle and top of canopy, respectively) were derived from the data collected in the N-trial; values indicated as triangles (Δ) were derived from the data collected in the T-trial at a leaf temperature of 25 °C.

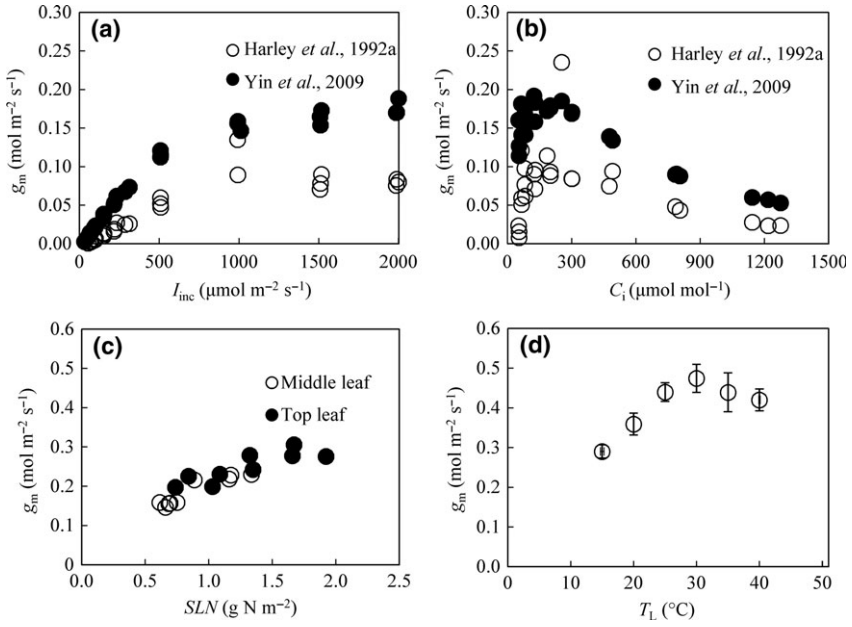

Fig. 4 Illustration of mesophyll conductance (g_m) in relation to changing incident irradiance (I_{inc}: Panel a), intercellular CO_2 concentration (C_i: Panel b), specific leaf nitrogen (*SLN*; Panel c) and leaf temperature (T_L; Panel d). In panels a and b, the data presented were obtained from the leaves at the middle of the canopy in the treatment without nitrogen fertilization in the N-trial; the open (○) and closed (●) circles were calculated using the variable *J* method of Harley *et al*. (1992a) (see Eqn 12 in the text) and the method of Yin *et al*. (2009) (see Eqn 13 in the text), respectively. In Panel c, the data presented were obtained at I_{inc} = 1000 μmol m^{-2} s^{-1} and C_a = 400 μmol mol^{-1} in the N-trial; the open (○) and closed (●) circles represent data obtained from leaves from the middle and the top of the canopy, respectively. In Panel d, the data presented were obtained at I_{inc} = 1000 μmol m^{-2} s^{-1} and C_a = 400 μmol mol^{-1} in the T-trial; the bars indicate standard errors of the mean (n = 3). Note the differences in scale along the y-axes.

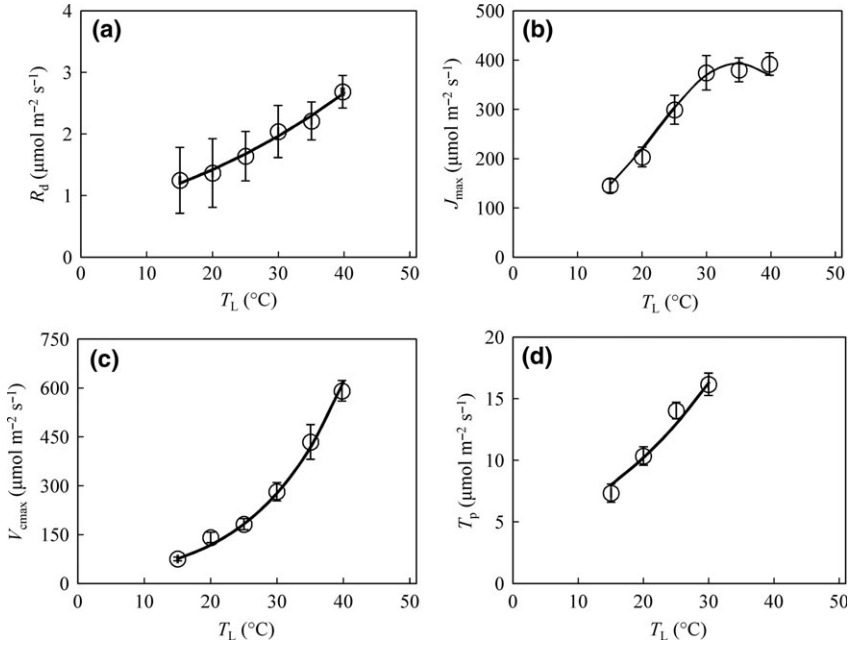

Fig. 5 Response of day respiration (R_d; Panel a), maximum potential linear e$^-$ transport rate (J_{max}; Panel b), maximum rate of carboxylation (V_{cmax}; Panel c) and the rate of triose phosphate export from the chloroplast (T_p; Panel d) to leaf temperature (T_L). The solid lines denote the predicted relations according to Eqn (6) or Eqn (7) with values presented in Table 1. The bars indicate standard errors of the mean (n = 3).

(κ_{2LL} = 0.21 mol mol^{-1}) or in the T-trial (κ_{2LL} = 0.37 mol mol^{-1}) (Fig. 6a, b). The *rRMSE* reduced significantly with decreasing value of κ_{2LL} until 0.13 mol mol^{-1} (Fig. 6c). Assuming κ_{2LL} = 0.13 mol mol^{-1} for the TN-trial, the r^2 and *rRMSE* were 0.94 and 26%, respectively; the error of model prediction distributed evenly across measured *SLN* and T_L (see Fig. S4).

Leaf photosynthetic competence of hemp in comparison with kenaf and cotton

Comparison of leaf photosynthetic competence of hemp with kenaf and cotton is presented in Fig. 7. The values of the main parameters are summarized in Table 1. In this illustration, we considered the uncertainty in estimated values of parameters (i.e. R_d, J_{max}, V_{cmax} and T_p) for their linear relationships with *SLN* and nonlinear relationships with T_L (presented as the shaded area). The modelled values of A for hemp are shown using lower and upper bounds of 95% confidence interval of these parameter values. Given that there was a large variation in the value of κ_{2LL} among different growth environments and each estimate of κ_{2LL} had a very small standard error (Table 1), the lower bounds were combined with κ_{2LL} of 0.21 mol mol^{-1} (derived from N-trial) while the upper bounds were combined with κ_{2LL} of 0.37 mol mol^{-1} (derived from T-trial).

For the response to C_i, these three crops had similar A at the current atmosphere CO_2 level (Fig. 7a). In case of a further increase in CO_2 level in the future, kenaf may become more productive than hemp. For both crops, there was a large uncertainty in the responses of A to I_{inc} and T_L (Fig. 7b, c) because these curves are affected by the value of κ_{2LL}. When using κ_{2LL} of 0.37 mol mol^{-1}, a value close to that of healthy C_3 leaves (presented as dashed black lines), the calculated A for hemp was similar to that for kenaf across different I_{inc} levels, but was slightly higher than for cotton at intermediate I_{inc}. Reducing κ_{2LL} to 0.21 mol mol^{-1} (presented as solid black lines) resulted in a reduction of A under light limiting condition and in a reduction of the optimal temperature. For the response to leaf nitrogen, the leaf photosynthetic competence of hemp, including its 95% confidence interval, was consistently higher than that of cotton and kenaf at *SLN* < 2.0 g N m^{-2}, which is close to the maximum *SLN* measured in this study (Fig. 7d).

Discussion

Hemp is considered an ideal annual crop for the bioeconomy as it has the potential to produce a high multipurpose biomass yield while requiring little inputs (Finnan & Burke, 2013; Tang *et al.*, 2016). However, very limited information is available on the physiological basis of hemp resource-use efficiency. With the aim of

 doi: 10.1111/gcbb.12451

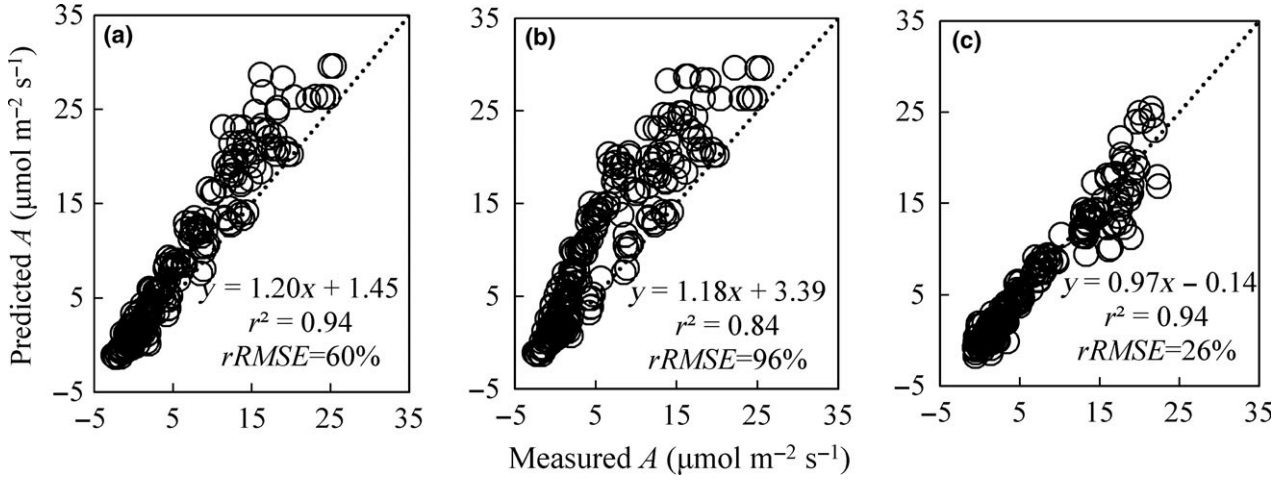

Fig. 6 Results of model validation against the data measured net photosynthesis rate (A) in the TN-trial. The dotted lines represent the 1:1 line. The predicted A values in panels a, b and c were with a value of κ_{2LL} = 0.21 mol mol^{-1} (derived from the N-trial), κ_{2LL} = 0.37 mol mol^{-1} (derived from the T-trial) and κ_{2LL} = 0.13 mol mol^{-1} (obtained by minimizing prediction error of A), respectively.

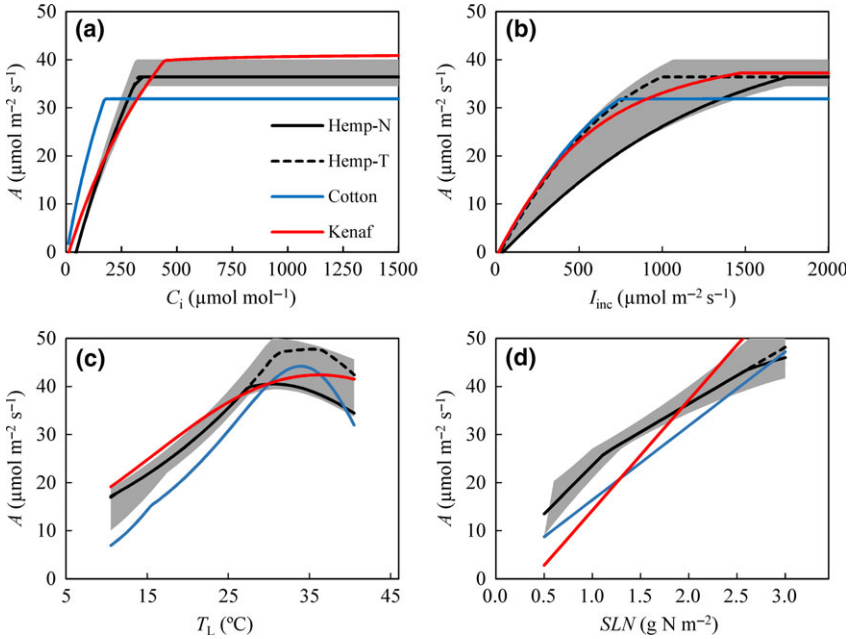

Fig. 7 Simulation of leaf photosynthetic capacity (A) of hemp (black lines), kenaf (red line) and cotton (blue line) in response to intercellular CO_2 concentration (C_i, Panel a), incident light intensity (I_{inc}, Panel b), leaf temperature (T_L, Panel c) and leaf nitrogen (SLN, Panel d). The hemp leaf photosynthesis presented by a continuous line was simulated with κ_{2LL} = 0.21 mol mol^{-1} (derived from the N-trial) while the dashed line was simulated with κ_{2LL} = 0.37 mol mol^{-1} (derived from the T-trial). The shaded area presents 95% confidence interval of hemp leaf photosynthesis. The photosynthesis rates of cotton were simulated using the model and values described in Harley *et al.* (1992b) while for kenaf the model and values came from Archontoulis *et al.* (2011). Except when used as the independent variable, the variables were set constant as C_a = 400 μmol mol^{-1}, I_{inc} = 2000 μmol m^{-2} s^{-1}, SLN = 2.0 g N m^{-2} and T_L = 25 °C.

understanding the response of leaf photosynthesis capacity of hemp to leaf nitrogen status and environmental factors and setting the basis for a hemp growth model, this study presents the results of extensive hemp leaf photosynthetic measurements and parameterization of a widely used photosynthesis model.

 doi: 10.1111/gcbb.12451

Table 1 List of model parameters (± standard errors if available) of hemp, cotton and kenaf

Parameter		Unit	Hemp	Cotton†	Kenaf§
Respiration					
R_d-*SLN*	Slope	μmol s^{-1} (g N)$^{-1}$	0.85 ± 0.15	0‡	0.80
	Intercept	μmol m^{-2} s^{-1}	0.03 ± 0.19	0.82‡	−0.37
E_{Rd}		J mol^{-1}	21634 ± 4085	84450	83440
e^- transport parameters					
J_{max}-*SLN*	Slope	μmol s^{-1} (g N)$^{-1}$	132.9 ± 14.6	98.1	122.1
	Intercept	μmol m^{-2} s^{-1}	54.4 ± 18.8	−4.6	−47.6
E_{Jmax}		J mol^{-1}	67292 ± 35986	79500	28149
D_{Jmax}		J mol^{-1}	114701 ± 28710	201000	474614‖
S_{Jmax}		J K^{-1} mol^{-1}	375 ± 82	650	1482‖
κ_{2LL}		mol mol^{-1}	0.21 ± 0.004 (N-trial) 0.37 ± 0.01 (T-trial)	0.24*	0.28
θ		-	0.70*	0.83*	0.63
Rubisco parameters					
V_{cmax}-*SLN*	Slope	μmol s^{-1} (g N)$^{-1}$	76.2 ± 9.8	60.0¶	66.7¶
	Intercept	μmol m^{-2} s^{-1}	12.6 ± 12.5	−9.6¶	26.0¶
E_{vcmax}		J mol^{-1}	63024 ± 1562	116300	61812
TPU parameters					
T_p-*SLN*	Slope	μmol s^{-1} (g N)$^{-1}$	4.2 ± 0.4	5.1¶	NA
	Intercept	μmol m^{-2} s^{-1}	4.3 ± 0.6	0.6¶	
E_{Tp}		J mol^{-1}	34417 ± 5298	53100	NA
g_m parameters					
δ		-	2.12 ± 0.09	NA	NA
g_{m0}		mol m^{-2} s^{-1}	0*	NA	NA

NA: not estimated or not available.

*Parameter values are fixed beforehand.

†Parameter values are derived from Harley *et al.* (1992b) with plants grown at an ambient [CO_2] of 35 Pa; the parameter values of temperature response are converted to fit Eqn (6) or Eqn (7) in the text; the value of θ is converted to fit Eqn (4) in the text.

‡R_d was held constant at different nitrogen levels and equal to 0.82 μmol m^{-2} s^{-1}.

§Parameter values are derived from Archontoulis *et al.* (2011). In their paper, the value of E_{Rd} is a function of *SLN*. The value presented here is derived at *SLN* = 2.0 g N m^{-2}. Slopes of R_d-*SLN* are calculated from simulation of R_d against *SLN* using original model.

¶Note that the absolute value of these parameters may be lower than the presented one when g_m is considered;

‖The optimum temperature J_{max} was not observed, so its J_{max} was fitted to the Arrhenius Eqn (6); thereby, D_{Jmax} and S_{Jmax} were not estimated. The presented value gave equal temperature sensitivities, but it was rejected by the authors due to a high standard error of the estimate.

Parameterization of the leaf photosynthesis model for hemp

Theoretically, the method to estimate R_d (day respiration) works best for the NPR (nonphotorespiratory) condition (Yin *et al.*, 2011). The estimated R_d in this study did not differ significantly between PR (photorespiratory) and NPR conditions ($P > 0.05$). This result suggests that estimating R_d from Eqn (9) is practicable even under PR condition (Yin *et al.*, 2009, 2011). Note that assessing the true R_d is somewhat difficult and the estimated R_d differs according to methodologies. A comparison of the method used in this study with other ones to estimate R_d is discussed in Yin *et al.* (2011). The estimated R_d values were on average 20% lower than R_{dk} values (respiration in the dark) in line with other reports (Brooks & Farquhar, 1985; Yin *et al.*, 2009, 2011). An *in vivo* metabolic study (Tcherkez *et al.*, 2005) indicated that the main inhibited steps were the entrance of hexose molecules into the glycolytic pathway and the Krebs cycle. Nevertheless, detailed mechanism of this difference still needs further research (Tcherkez *et al.*, 2012).

Both R_d and R_{dk} increased monotonically with an increase in *SLN* and T_L (Figs 2, 3 and 5) within the tested ranges. The result agrees with those of Yin *et al.*

 doi: 10.1111/gcbb.12451

(2009, 2011), but does not support those in Harley *et al.* (1992b) for cotton, where a constant R_d was considered at changing nitrogen and temperature. For hemp, Chandra *et al.* (2008, 2011a) reported that R_{dk} levelled off or slightly decreased with an increase in temperature from 30 to 40 °C. This was not confirmed in the present study, although the highest R_{dk} measured at 25 °C in our study is comparable with the value observed in Chandra *et al.* (2008, 2011a). The reason for such discrepancy of R_{dk} in response to T_L is not clear. It is probably due to an artefact of different protocols or due to changes in thermal sensitivity of respiration at different growth environments and plant status (e.g. drought, nutrient availability and sugar concentration) (Atkin *et al.*, 2005; Katja *et al.*, 2012). If an increase of respiration with increasing *SLN* and T_L is proven for hemp, it could counteract, at least partly, the positive effects of *SLN* and T_L on *A* (net photosynthesis rate) when considering at daily basis.

Based on the findings that the maximum quantum yields (the initial slopes of the response of CO_2 uptake to photon absorption) were conserved across age classes within species or across the mature photosynthetic organs of different species (Long *et al.*, 1993), κ_{2LL} was often fixed as a constant across different growth environments and species in studies of plant photosynthesis (Harley *et al.*, 1992b; Medlyn *et al.*, 2002). However, very different values have been assumed in different studies without clear explanation, ranging from 0.18 mol mol^{-1} until 0.39 mol mol^{-1} (Harley *et al.*, 1992b; Wullschleger, 1993; Medlyn *et al.*, 2002; Yamori *et al.*, 2010). The estimated κ_{2LL} in the present study did not change with *SLN* and with T_L, but it was not constant across growth environments (0.21 mol mol^{-1} for the N-trial; 0.37 mol mol^{-1} for the T-trial and 0.13 mol mol^{-1} resulted in the best prediction of measurements in the TN-trial), in line with Archontoulis *et al.* (2011) who observed that cardoon (*Cynara cardunculus*) had a higher κ_{2LL} in the cold season than in the warm season. The reason for the variation in κ_{2LL} in different environments is still not fully understood. We speculate that the low κ_{2LL} in the N-trial and the TN-trial in comparison with the κ_{2LL} in the T-trial is a consequence of photoinhibition that occurs naturally in field plants grown in West Europe when the temperature is low and the sky is clear (Long *et al.*, 1994). The plants of the N-trial and the TN-trial were grown outdoors, with fluctuations in temperature and irradiance; particularly, the plants in the TN-trial experienced a sudden drop of temperature five days before measuring (Fig. S1). These conditions could have resulted in severe photoinhibition (Long *et al.*, 1983; Powles *et al.*, 1983) causing a reduction in Φ_{2LL} (PSII quantum use efficiency under strictly limiting light) and an increase in the fraction of alternative electron transport (i.e. $\frac{f_{pseudo(b)}}{1-f_{cyc}}$; cf. Eqn 9a) (Curwiel & Van Rensen, 1993; Murata *et al.*, 2012), hence a low κ_{2LL}. In contrast, the plants of the T-trial were grown in the glasshouse where both light intensity and temperature were controlled at a condition free of photoinhibition. Thus, the value of κ_{2LL} (0.37 mol mol^{-1}) was high and close to the range for healthy C_3 leaves (between 0.32 mol mol^{-1} and 0.35 mol mol^{-1}) (Hikosaka *et al.*, 2016 and their references). Moreover, the variation in κ_{2LL} could be partly attributed to the change in β (leaf absorbance; cf. Eqn 9a) as a result of environmental acclimation (Archontoulis *et al.*, 2011). A higher β in the T-trial than in the N-trial and the NT-trial is reflected by the higher *SPAD* values when considered at the same *SLN* (Fig. S5). Given that the value of κ_{2LL} varied significantly across different environments and that it affected significantly the prediction of photosynthesis when electron transport was limited (i.e. A_j) (Fig. 7), caution is needed when modelling photosynthesis rate using a value of κ_{2LL} derived from different environments, particularly if these include both glasshouse and open field conditions. To improve modelling of crop growth in field conditions, further study should be conducted to investigate the mechanisms underlying variation in κ_{2LL} during the whole growth season.

The relationships J_{max}-*SLN*, V_{cmax}-*SLN* and T_p-*SLN* were consistent across canopy positions and growth environments whereas linear regression of these relationships resulted in negative intersections at the *x-axis* (Fig. 3), in line with Akita *et al.* (2012) but different from Archontoulis *et al.* (2011) and Braune *et al.* (2009) where the intersection of linear extrapolating resulted in a minimum *SLN* required for photosynthesis (SLN_b). Given that it is not physiologically possible to have a negative SLN_b, the results in this study indicate that the relationships J_{max}-*SLN*, V_{cmax}-*SLN* and T_p-*SLN* for hemp may not be perfectly linear. Further study would be needed to elucidate the relationship between these parameters and *SLN* at *SLN* levels approaching zero.

It is well recognized that g_m is not infinite (Bernacchi *et al.*, 2002). Using both the variable *J* method and the modelling method, our analysis for hemp (Fig. 4) supports that g_m varies with changing C_i and I_{inc} (Flexas *et al.*, 2007, 2012; Yin *et al.*, 2009), which is in contrast with the assumption that g_m is independent of C_i and I_{inc} (Bernacchi *et al.*, 2002). This highlights an important uncertainty in the present understanding of CO_2 diffusion processes in leaves. The g_m obtained from Eqn (13) with a constant δ changed in line with *A* (cf. Figs 2 and 4), confirming the assumption of Piel *et al.* (2002) and Ethier *et al.* (2006) that g_m is correlated with *A*. The value of δ (2.12) is lower than that of wheat (2.54) (Yin *et al.*, 2009) but higher than that of rice (0.45~1.57) (Gu *et al.*, 2012).

Does hemp have high photosynthetic competence?

The observed A_{max} was observed to be levelled off at 25–35 °C (Fig. 2d) that is comparable with the 27 °C reported in Cosentino *et al.* (2012) and the 30 °C reported in Chandra *et al.* (2011a) for hemp leaf photosynthesis. The wide range of optimal temperature for leaf photosynthesis confirms the fact that hemp has been cultivated from the tropic (Tang *et al.*, 2012) to the polar circle (Pahkala *et al.*, 2008).

The highest A_{max} (light-saturated net photosynthesis rate) at 25 °C was measured at 31.2 ± 1.9 μmol m^{-2} s^{-1} (Fig. 2b). This value is higher than the highest value reported for hemp in De Meijer *et al.* (1995) and (Chandra *et al.*, 2008, 2011a), which were 19.0 μmol m^{-2} s^{-1} and 24.0 μmol m^{-2} s^{-1}, respectively. The highest A_{max} in this study is comparable with that of other C_3 bioenergy crops. Archontoulis *et al.* (2011) reported that the highest A_{max} of kenaf, sunflower (*Helianthus annuus* L.) and cardoon ranged between 30 μmol m^{-2} s^{-1} and 35 μmol m^{-2} s^{-1} under optimum temperature.

As direct comparison of A_{max} among crops is difficult due to the variation in experimental protocols and plant status, we constructed *A*-C_i, *A*-I_{inc}, *A*-T_L and *A*-*SLN* curves for hemp, cotton and kenaf with the same values of variables (i.e. C_i, I_{inc}, T_L and *SLN*) (Fig. 7). The comparison highlighted that hemp has higher leaf photosynthesis rate than cotton and kenaf at a low nitrogen condition (i.e. *SLN* < 2.0 g N m^{-2}). This was presumably because hemp has a relatively low SLN_b. Analysis of newly senesced hemp leaves resulted in a nitrogen content of 0.25 ± 0.01 g N m^{-2}. This value is at the low range of SLN_b among C_3 crops and weeds (average value = 0.31 ± 0.03 g N m^{-2}) and is considerably lower than the estimation for kenaf (0.39 ± 0.13 g N m^{-2}) (Archontoulis *et al.*, 2011).

The high photosynthesis rate of hemp at low nitrogen condition is in line with its observed high productivity at low nitrogen input (Struik *et al.*, 2000; Finnan & Burke, 2013) and puts hemp ahead of cotton and kenaf from a perspective of bio-economy. However, our model approach has limitations. Firstly, the comparison was based on parameters derived from different studies conducted in different environments. Secondly, even though the FvCB model is biochemically based and the relationships J_{max}-*SLN*, V_{cmax}-*SLN* and T_p-*SLN* were consistent in this study across canopy positions and growth environments (Fig. 3), increasing evidences show that the model parameters may change when plant acclimates to growing environments. For example, Harley *et al.* (1992b) reported that the slope of V_{cmax}-*SLN* decreased with an increase in CO_2 concentration in the growth environment. The present study also indicated that the value of κ_{2LL} may differ among growth environments. Thirdly, variation in photosynthetic competence among cultivars has been reported for hemp (Chandra *et al.*, 2011b). As only one cultivar was studied, it is not clear whether the advantage of photosynthetic competence of hemp is persistent across cultivars. Therefore, to consolidate the potential of hemp as a bio-economic sustainable crop, further study is needed to compare hemp leaf photosynthetic competence with those of cotton, kenaf and other bioenergy crops in the same growing environment with multiple cultivars.

Acknowledgements

The research leading to these results has received funding from the European Union's Seventh Framework Programme for research, technological development and demonstration under grant agreement no 311849.

References

Akita R, Kamiyama C, Hikosaka K (2012) Polygonum sachalinense alters the balance between capacities of regeneration and carboxylation of ribulose-1,5-bisphosphate in response to growth CO_2 increment but not the nitrogen allocation within the photosynthetic apparatus. *Physiologia Plantarum*, **146**, 404–412.

Alexopoulou E, Li D, Papatheohari Y *et al.* (2015) How kenaf (*Hibiscus cannabinus* L.) can achieve high yields in Europe and China. *Industrial Crops and Products*, **68**, 131–140.

Allegret S (2013) The history of hemp. In: *Hemp: Industrial Production and Uses* (eds Allegret S, Bouloc P, Arnaud L), pp. 4–26. CPi Group (UK) Ltd, Croydon, UK.

Amaducci S, Errani M, Venturi G (2002) Response of hemp to plant population and nitrogen fertilisation. *Italian Journal of Agronomy*, **6**, 103–111.

Amaducci S, Scordia D, Liu FH *et al.* (2015) Key cultivation techniques for hemp in Europe and China. *Industrial Crops and Products*, **68**, 2–16.

Archontoulis SV, Yin X, Vos J *et al.* (2011) Leaf photosynthesis and respiration of three bioenergy crops in relation to temperature and leaf nitrogen: how conserved are biochemical model parameters among crop species? *Journal of Experimental Botany*, **63**, 895–911.

Atkin OK, Bruhn D, Hurry VM *et al.* (2005) The hot and the cold: unravelling the variable response of plant respiration to temperature. *Functional Plant Biology*, **32**, 87–105.

Barth M, Carus M (2015) *Carbon Footprint and Sustainability of Different Natural Fibres for Biocomposites and Insulation Material*, Hürth, Germany, nova-Institute. Available at: http://bio-based.eu/ecology/ (accessed 24 January 2017).

Bellasio C, Beerling DJ, Griffiths H (2015) An Excel tool for deriving key photosynthetic parameters from combined gas exchange and chlorophyll fluorescence: theory and practice. *Plant, Cell and Environment*, **69**, 80–97.

Bernacchi CJ, Portis AR, Nakano H *et al.* (2002) Temperature response of mesophyll conductance. Implications for the determination of Rubisco enzyme kinetics and for limitations to photosynthesis in vivo. *Plant Physiology*, **130**, 1992–1998.

Bertoli A, Tozzi S, Pistelli L *et al.* (2010) Fibre hemp inflorescences: from crop-residues to essential oil production. *Industrial Crops and Products*, **32**, 329–337.

Bouloc P, Van der Werf HMG (2013) The role of hemp in sustainable development. In: *Hemp: Industrial Production and Uses* (eds Bouloc P, Allegret S, Arnaud L), pp. 278–289. CPi Group (UK) Ltd, Croydon, UK.

Bouman BAM, Feng L, Tuong TP *et al.* (2007) Exploring options to grow rice using less water in northern China using a modelling approach: II. Quantifying yield, water balance components, and water productivity. *Agricultural Water Management*, **88**, 23–33.

Braune H, Müller J, Diepenbrock W (2009) Integrating effects of leaf nitrogen, age, rank, and growth temperature into the photosynthesis-stomatal conductance model LEAFC3-N parameterised for barley (*Hordeum vulgare* L.). *Ecological Modelling*, **220**, 1599–1612.

Brooks A, Farquhar GD (1985) Effect of temperature on the CO_2/O_2 specificity of ribulose-1,5-bisphosphate carboxylase/oxygenase and the rate of respiration in the light. *Planta*, **165**, 397–406.

Busch FA, Sage RF (2016) The sensitivity of photosynthesis to O_2 and CO_2 concentration identifies strong Rubisco control above the thermal optimum. *New Phytologist*, **213**, 1036–1051.

Carus M, Sarmento L (2016) *The European Hemp Industry: Cultivation, processing and applications for fibres, shivs and seeds*. pp 1-9, European Industrial Hemp Association (EIHA), Hürth, Germany. Available at: http://eiha.org/media/2016/05/16-05-17-European-Hemp-Industry-2013.pdf (accessed 24 January 2017).

 doi: 10.1111/gcbb.12451

Carus M, Karst S, Kauffmann A *et al.* (2013) *The European Hemp Industry: Cultivation, processing and applications for fibres, shivs and seeds*. European Industrial Hemp Association (EIHA), Hürth, Germany. Available at : http://eiha.org/media/2014/10/13-06-European-Hemp-Industry.pdf (accessed 24 January 2017).

Chandra S, Lata H, Khan IA *et al.* (2008) Photosynthetic response of *Cannabis sativa* L. to variations in photosynthetic photon flux densities, temperature and CO2 conditions. *Physiology and Molecular Biology of Plants*, **14**, 299–306.

Chandra S, Lata H, Khan IA *et al.* (2011a) Temperature response of photosynthesis in different drug and fiber varieties of *Cannabis sativa* L. *Physiology and Molecular Biology of Plants*, **17**, 297–303.

Chandra S, Lata H, Khan IA *et al.* (2011b) Photosynthetic response of Cannabis sativa L., an important medicinal plant, to elevated levels of CO_2. *Physiology and Molecular Biology of Plants*, **17**, 291–295.

Chandra S, Lata H, Mehmedic Z *et al.* (2015) Light dependence of photosynthesis and water vapor exchange characteristics in different high Δ9-THC yielding varieties of *Cannabis sativa* L. *Journal of Applied Research on Medicinal and Aromatic Plants*, **2**, 39–47.

Cosentino SL, Testa G, Scordia D *et al.* (2012) Sowing time and prediction of flowering of different hemp (*Cannabis sativa* L.) genotypes in southern Europe. *Industrial Crops and Products*, **37**, 20–33.

Curwiel VB, Van Rensen JJS (1993) Influence of photoinhibition on electron transport and photophosphorylation of isolated chloroplasts. *Physiologia Plantarum*, **89**, 97–102.

De Meijer EPM, Van der Werf HMG (1994) Evaluation of current methods to estimate pulp yield of hemp. *Industrial Crops and Products*, **2**, 111–120.

De Meijer WJM, Van Der Werf HMG, Mathijssen EWJM, Van Den Brink PWM (1995) Constraints to dry matter production in fibre hemp (*Cannabis sativa* L.). *European Journal of Agronomy*, **4**, 109–117.

Ethier G, Livingston N, Harrison D, *et al.* (2006) Low stomatal and internal conductance to CO_2 versus Rubisco deactivation as determinants of the photosynthetic decline of ageing evergreen leaves. *Plant, Cell and Environment*, **29**, 2168–2184.

Farquhar GD, Von Caemmerer S, Berry JA (1980) A biochemical model of photosynthetic CO_2 assimilation in leaves of C_3 species. *Planta*, **149**, 78–90.

Finnan J, Burke B (2013) Nitrogen fertilization to optimize the green gas balance of hemp crops grown for biomass. *GCB Bioenergy*, **5**, 701–712.

Flexas J, Diaz-Espejo A, Galmes J *et al.* (2007) Rapid variations of mesophyll conductance in response to changes in CO_2 concentration around leaves. *Plant, Cell and Environment*, **30**, 1284–1298.

Flexas J, Barbour MM, Brendel O *et al.* (2012) Mesophyll diffusion conductance to CO_2: an unappreciated central player in photosynthesis. *Plant Science*, **193**, 70–84.

Gu JF, Yin XY, Stomph TJ *et al.* (2012) Physiological basis of genetic variation in leaf photosynthesis among rice (*Oryza sativa* L.) introgression lines under drought and well-watered conditions. *Journal of Experimental Botany*, **63**, 5137–5153.

Harley PC, Loreto F, Di Marco G *et al.* (1992a) Theoretical considerations when estimating the mesophyll conductance to CO_2 flux by analysis of the response of photosynthesis to CO_2. *Plant Physiology*, **98**, 1429–1436.

Harley PC, Thomas RB, Reynolds JF *et al.* (1992b) Modelling photosynthesis of cotton grown in elevated CO_2. *Plant, Cell and Environment*, **15**, 271–282.

Hikosaka K, Noguchi K, Terashima I (2016) Modeling leaf gas exchange. In:*Canopy Photosynthesis: From Basics to Applications* (eds Hikosaka K, Niinemets Ü, Anten NPR), pp. 61–100. Springer, London, UK.

Jordan N, Boody G, Broussard W *et al.* (2007) Sustainable development of the agricultural bio-economy. *Science*, **316**, 1570–1571.

Katja H, Irina B, Hiie I *et al.* (2012) Temperature responses of dark respiration in relation to leaf sugar concentration. *Physiologia Plantarum*, **144**, 320–334.

Kreuger E, Prade T, Escobar F *et al.* (2011) Anaerobic digestion of industrial hemp–Effect of harvest time on methane energy yield per hectare. *Biomass and Bioenergy*, **35**, 893–900.

Lips SJJ, van Dam JEG (2013) Kenaf fibre crop for bioeconomic industrial development. In: *Kenaf: A Multi-Purpose Crop for Several Industrial Applications* (eds Monti A, Alexopoulou E), pp. 105–143. Springer, London, UK.

Long S, East T, Baker N (1983) Chilling damage to photosynthesis in young *Zea mays* I. Effects of light and temperature variation on photosynthetic CO_2 assimilation. *Journal of Experimental Botany*, **34**, 177–188.

Long S, Postl WF, Bolhár-Nordenkampf HR (1993) Quantum yields for uptake of carbon dioxide in C_3 vascular plants of contrasting habitats and taxonomic groupings. *Planta*, **189**, 226–234.

Long S, Humphries S, Falkowski PG (1994) Photoinhibition of photosynthesis in nature. *Annual Review of Plant Biology*, **45**, 633–662.

Marija M, Māra V, Veneranda S (2011) Changes of photosynthesis-related parameters and productivity of *Cannabis sativa* under different nitrogen supply. *Environmental and Experimental Biology*, **9**, 61–69.

Mccormick K, Kautto N (2013) The bioeconomy in Europe: an overview. *Sustainability*, **5**, 2589–2608.

Medlyn BE, Dreyer E, Ellsworth D *et al.* (2002) Temperature response of parameters of a biochemically based model of photosynthesis. II. A review of experimental data. *Plant, Cell and Environment*, **25**, 1167–1179.

Murata N, Allakhverdiev SI, Nishiyama Y (2012) The mechanism of photoinhibition in vivo: re-evaluation of the roles of catalase, α-tocopherol, non-photochemical quenching, and electron transport. *Biochimica et Biophysica Acta (BBA) - Bioenergetics*, **1817**, 1127–1133.

Ögren E, Evans J (1993) Photosynthetic light-response curves. *Planta*, **189**, 182–190.

Oomah BD, Busson M, Godfrey DV, Drover JCG (2002) Characteristics of hemp (*Cannabis sativa* L.) seed oil. *Food Chemistry*, **76**, 33–43.

Pahkala K, Pahkala E, Syrjala H (2008) Northern limits to fiber hemp production in Europe. *Journal of Industrial Hemp*, **13**, 104–116.

Patanè C, Cosentino SL (2013) Yield, water use and radiation use efficiencies of kenaf (*Hibiscus cannabinus* L.) under reduced water and nitrogen soil availability in a semi-arid Mediterranean area. *European Journal of Agronomy*, **46**, 53–62.

Piel C, Frak E, Le Roux X *et al.* (2002) Effect of local irradiance on CO_2 transfer conductance of mesophyll in walnut. *Journal of Experimental Botany*, **53**, 2423–2430.

Powles SB, Berry JA, Bjorkman O (1983) Interaction between light and chilling temperature on the inhibition of photosynthesis in chilling-sensitive plants. *Plant, Cell and Environment*, **6**, 117–123.

Prade T, Svensson S-E, Andersson A *et al.* (2011) Biomass and energy yield of industrial hemp grown for biogas and solid fuel. *Biomass and Bioenergy*, **35**, 3040–3049.

Rice B (2008) Hemp as a feedstock for biomass-to-energy conversion. *Journal of Industrial Hemp*, **13**, 145–156.

Sage RF, Kubien DS (2007) The temperature response of C_3 and C_4 photosynthesis. *Plant, Cell and Environment*, **30**, 1086–1106.

Salentijn EMJ, Zhang Q, Amaducci S *et al.* (2015) New developments in fiber hemp (*Cannabis sativa* L.) breeding. *Industrial Crops and Products*, **68**, 32–41.

Sharkey TD, Bernacchi CJ, Farquhar GD *et al.* (2007) Fitting photosynthetic carbon dioxide response curves for C_3 leaves. *Plant, Cell and Environment*, **30**, 1035–1040.

Sinclair TR, Horie T (1989) Leaf nitrogen, photosynthesis, and crop radiation use efficiency: a review. *Crop Science*, **29**, 90–98.

Struik PC, Amaducci S, Bullard MJ *et al.* (2000) Agronomy of fibre hemp (*Cannabis sativa* L.) in Europe. *Industrial Crops and Products*, **11**, 107–118.

Tang Z, Hu X, Sun T *et al.* (2012) Adaptability of different hemp varieties (lines) in Xishuangbanna prefecture. *Journal of Southern Agriculture*, **43**, 160–163. (Chinese with English abstract).

Tang K, Struik PC, Yin X *et al.* (2016) Comparing hemp (*Cannabis sativa* L.) cultivars for dual-purpose production under contrasting environments. *Industrial Crops and Products*, **87**, 33–44.

Tcherkez G, Cornic G, Bligny R *et al.* (2005) In vivo respiratory metabolism of illuminated leaves. *Plant Physiology*, **138**, 1596–1606.

Tcherkez G, Boex-Fontvieille E, Mahé A *et al.* (2012) Respiratory carbon fluxes in leaves. *Current Opinion in Plant Biology*, **15**, 308–314.

Von Caemmerer S, Farquhar G, Berry J (2009) Biochemical model of C_3 photosynthesis. In: *Photosynthesis In Silico* (eds Laisk A, Nedbal L, Govindjee), pp. 209–230. Springer, London, UK.

Wirtshafter DE (2004) Ten years of a modern hemp industry. *Journal of Industrial Hemp*, **9**, 9–14.

Wullschleger SD (1993) Biochemical limitations to carbon assimilation in C_3 plants: a retrospective analysis of the A/C_i curves from 109 species. *Journal of Experimental Botany*, **44**, 907–920.

Yamori W, Evans JR, Von Caemmerer S (2010) Effects of growth and measurement light intensities on temperature dependence of CO_2 assimilation rate in tobacco leaves. *Plant, Cell and Environment*, **33**, 332–343.

Yin XY, Struik PC (2009) C_3 and C_4 photosynthesis models: an overview from the perspective of crop modelling. *NJAS - Wageningen Journal of Life Sciences*, **57**, 27–38.

Yin XY, Van Laar HH (2005) *Crop Systems Dynamics: An Ecophysiological Simulation Model for Genotype-by-Environment Interactions*. Wageningen, Wageningen Academic.

Yin XY, Harbinson J, Struik PC (2006) Mathematical review of literature to assess alternative electron transports and interphotosystem excitation partitioning of steady-state C-3 photosynthesis under limiting light. *Plant Cell and Environment*, **29**, 1771–1782.

Yin XY, Struik PC, Romero P *et al.* (2009) Using combined measurements of gas exchange and chlorophyll fluorescence to estimate parameters of a biochemical C_3 photosynthesis model: a critical appraisal and a new integrated approach applied to leaves in a wheat (*Triticum aestivum* L.) canopy. *Plant, Cell and Environment*, **32**, 448–464.

Yin XY, Sun ZP, Struik PC *et al.* (2011) Evaluating a new method to estimate the rate of leaf respiration in the light by analysis of combined gas exchange and chlorophyll fluorescence measurements. *Journal of Experimental Botany*, **62**, 3489–3499.

Supporting Information

Additional Supporting Information may be found online in the supporting information tab for this article:

Figure S1. The daily temperature and global radiation during the period from sowing to the end of the experiment for plants grown in the open field (i.e. TN-trial in 2013 and N-trial in 2014).
Figure S2. Dependence of lumped parameter (*s*) in Eqn (9) on leaf nitrogen (*SLN*) and dependence of the efficiency of converting incident irradiance into linear electron transport under limiting light (κ_{2LL}) on *SLN* and leaf temperature (T_L).
Figure S3. The estimated day respiration under photorespiratory condition, i.e. at 21% O_2 against that under non-photorespiratory condition, i.e. at 2% O_2.
Figure S4. The error of model validation against leaf nitrogen (*SLN*) and temperature (T_L).
Figure S5. The effect of growth environment on the relationship between *SPAD* values and leaf nitrogen (*SLN*).

 doi: 10.1111/gcbb.12451